Interconnection of nitrogen fixers and iron in the Pacific Ocean: Theory and numerical simulations

S. Dutkiewicz,[1] B. A. Ward,[1] F. Monteiro,[2] and M. J. Follows[1]

Received 10 January 2011; revised 16 August 2011; accepted 6 November 2011; published 26 January 2012.

[1] We examine the interplay between iron supply, iron concentrations and phytoplankton communities in the Pacific Ocean. We present a theoretical framework which considers the competition for iron and nitrogen resources between phytoplankton to explain where nitrogen fixing autotrophs (diazotrophs, which require higher iron quotas, and have slower maximum growth) can co-exist with other phytoplankton. The framework also indicates that iron and fixed nitrogen concentrations can be strongly controlled by the local phytoplankton community. Together with results from a three-dimensional numerical model, we characterize three distinct biogeochemical provinces: 1) where iron supply is very low diazotrophs are excluded, and iron-limited nondiazotrophic phytoplankton control the iron concentrations; 2) a transition region where nondiazotrophic phytoplankton are nitrogen limited and control the nitrogen concentrations, but the iron supply is still too low relative to nitrate to support diazotrophy; 3) where iron supplies increase further relative to the nitrogen source, diazotrophs and other phytoplankton coexist; nitrogen concentrations are controlled by nondiazotrophs and iron concentrations are controlled by diazotrophs. The boundaries of these three provinces are defined by the rate of supply of iron relative to the supply of fixed nitrogen. The numerical model and theory provide a useful tool to understand the state of, links between, and response to changes in iron supply and phytoplankton community structure that have been suggested by observations.

Citation: Dutkiewicz, S., B. A. Ward, F. Monteiro, and M. J. Follows (2012), Interconnection of nitrogen fixers and iron in the Pacific Ocean: Theory and numerical simulations, *Global Biogeochem. Cycles*, *26*, GB1012, doi:10.1029/2011GB004039.

1. Introduction

[2] The ecology and biogeochemistry of the world's oceans are complex and tightly interconnected. Microbial community structure is shaped by the variable physical, chemical and predatory environment [*Margalef*, 1968] including a strong "bottom up" influence due to resource supply. For example, opportunistic diatoms often dominate upwelling regimes with a high supply of nutrients, and specialized gleaners including the picocyanobacteria dominate communities in the oligotrophic subtropical gyres. In particular, nitrogen fixers (diazotrophs), which provide most of the exogenous nitrogen to the global ocean, appear to be strongly influenced by the nutrient environment with a particularly important role for iron [*Falkowski*, 1997].

[3] Iron occurs in the ocean at very low concentrations, yet is an essential component of nitrogenase, the enzyme used to break the triple bond of dinitrogen gas. Regulation of diazotroph activity by iron has been inferred in the field [*Moore et al.*, 2009; *Mills et al.*, 2004; *Berman-Frank et al.*, 2007]. The modulation of global nitrogen fixation by variations in the aeolian supply of iron has been illustrated in sensitivity studies using numerical models [*Moore and Doney*, 2007; *Moore et al.*, 2006; *Krishnamurthy et al.*, 2009; *Monteiro et al.*, 2011]. In these models the strength of the external source of iron to the ocean is positively correlated with global nitrogen fixation rates and, consequently, primary production. The aeolian iron supply has changed markedly across the last glacial maximum [*Mahowald et al.*, 2006], pre-industrial and modern day [*Luo et al.*, 2008; *Mahowald et al.,* 2009] and is likely to change in the future [*Mahowald and Luo*, 2003; *Tegen et al.*, 2004].

[4] These field and model studies indicate relationships between iron, nitrogen fixation and productivity. How is this complex biogeochemical system organized? Can we predict and interpret the observations and complex numerical model results using transparent and idealized models? Here we seek to underpin these suggested relationships with a mechanistic and quantitative theoretical framework. Community structure responds to changes in the supply of limiting nutrients (e.g., iron fertilization [*Boyd et al.*, 2007; *de Baar et al.*, 2005]) and, at the same time, microbial communities mediate marine biogeochemical cycles. Resource competition theory [*Tilman*, 1977, 1982] (discussed further in section 2) provides a framework which connects community composition and the resource environment. In a recent study of a global ocean model [*Dutkiewicz et al.*, 2009] the ambient concentration of the limiting resource concentration in the oligotrophic tropics and subtropics was shown to be a function of the physiology of the dominant plankton types,

[1]Department of Earth, Atmospheric and Planetary Sciences, Massachusetts Institute of Technology, Cambridge, Massachusetts, USA.
[2]School of Geographical Sciences, University of Bristol, Bristol, UK.

0886-6236/12/2011GB004039

consistent with the predictions of resource competition theory. That study, however, did not represent nitrogen fixing phytoplankton. In a similar model which did explicitly resolved diverse types of diazotrophs, capturing observed distributions [*Monteiro et al.*, 2010], their habitat was found to be restricted to regions with low fixed nitrogen concentrations and sufficient iron and phosphate [*Monteiro et al.*, 2011], also broadly consistent with resource competition concepts, though the complex relationships between sources of nitrogen, iron and community structure were not fully developed.

[5] Here we extend that perspective to provide a simple, yet powerful, mechanistic description of how the iron supply controls nitrogen fixation in the ocean and, in turn, how iron concentrations are biologically modulated. We apply concepts from resource competition theory [*Tilman*, 1977, 1982], extending the approach of *Dutkiewicz et al.* [2009] to include diazotrophs. The theoretical framework (section 2) provides a formal, mechanistic description of the controls on modeled diazotroph habitat and explains the coexistence (or lack thereof) of diazotrophs and other phytoplankton. In section 3 we describe the numerical physical-biogeochemical-ecosystem model that includes diazotroph and several nondiazotroph phytoplankton functional types. We then present a series of numerical simulations (sections 4 and 5) and use the theoretical framework to understand the model responses to changes in key physiological parameters and aeolian supply of iron. We examine the complex, and regionally specific, interactions between community structure and iron supply (section 6). Here we focus our study on contrasts in the model Pacific ocean which has large areas of both iron and nitrogen limited productivity, unlike the Atlantic which is largely nitrogen limited.

2. Theoretical Framework

[6] Resource competition theory [*Tilman*, 1977, 1982] provides a framework for interpreting the relationship between organisms and their resource environment. Here we recap some essential elements of the theory based on the highly simplified assumption of a local balance between growth and loss where the physical transport of organisms can be neglected. We consider a system with two nutrients (fixed nitrogen, N, and iron, Fe), a nondiazotrophic phytoplankton type (P_P) and an autotrophic diazotroph (P_D):

$$\frac{dP_P}{dt} = \mu_P \min\left(\frac{N}{N+\kappa_{NP}}, \frac{Fe}{Fe+\kappa_{FeP}}\right) P_P - m_P P_P \quad (1)$$

$$\frac{dP_D}{dt} = \mu_D \frac{Fe}{Fe+\kappa_{FeD}} P_D - m_D P_D \quad (2)$$

$$\frac{dN}{dt} = -\mu_P \min\left(\frac{N}{N+\kappa_{NP}}, \frac{Fe}{Fe+\kappa_{FeP}}\right) P_P + m_D P_D + S_N \quad (3)$$

$$\frac{dFe}{dt} = -\mu_P \min\left(\frac{N}{N+\kappa_{NP}}, \frac{Fe}{Fe+\kappa_{FeP}}\right) R_P P_P - \mu_D \frac{Fe}{Fe+\kappa_{FeD}} R_D P_D + S_{Fe}. \quad (4)$$

[7] Here μ_j ($j = P,D$) is the maximum growth rate (and could be a function of light and temperature). Nutrient limitation of growth is parameterized as a Monod function where κ_{ij} ($i = N,Fe$) is the growth half-saturation constant. Nondiazotrophs are assumed to follow a Liebig's law of the minimum response to limitation by either iron or fixed nitrogen. For simplicity diazotrophs are assumed to fix all the nitrogen that they require, and that their growth is only limited by iron. Loss rate, m_j is a simple linear representation of sinking, grazing, viral lysis and other loss processes. The cellular iron-to-nitrogen ratio is given by R_j and is assumed here to be fixed, though we note that the model could be recast in a variable quota system [cf. *Tilman*, 1977; *Verdy et al.*, 2009]. S_i is the local source (and sink) of the nutrient, including ocean transport, remineralization of organic matter, any other outside sources (such as dust supply), and sinks such as iron scavenging or denitrification. We assume that part of the organic matter lost by mortality/grazing by nondiazotrophs and the iron from diazotrophs will remineralize locally and become part of the source term S_i. However, to emphasize that the nitrogen fixed by the diazotrophs is a source of new nitrogen to the system, we have an explicit term $m_D P_D$ as a source of N in equation (3). Though informative, this assumption is not essential for the discussion here.

[8] Since the energetic cost of breaking the triple bond of N_2 is large we can assume that diazotrophs have a lower maximum growth rate than the nondiazotrophs ($\mu_D < \mu_P$), consistent with laboratory cultures [e.g., *LaRoche and Breitbarth*, 2005; *Goebel et al.*, 2008]. As diazotrophs also have a higher requirement for iron (required for nitrogenase [*Kustka et al.*, 2003]), we assume that $R_D > R_P$. As formulated here and following from work by *Verdy et al.* [2009] these elemental ratios also imply $\kappa_{FeD} > \kappa_{FeP}$.

[9] Here, for simplicity, we neglect other nutrients (e.g. phosphorus), though the framework could be extended to include additional nutrients. We could also incorporate diazotroph's ability to consume fixed nitrogen as well as fixing their own (see Appendix A), however this does not qualitatively affect the results presented here.

2.1. Competition for Resources

[10] According to Tilman's theory, the equilibrium fitness of a phytoplankton class j, for resource i, is defined by its equilibrium requirement for the limiting resource. This is the concentration of the limiting resource i at which the growth of organism j is balanced by mortality [*Tilman*, 1982]. These equilibrium nutrient solutions are found by setting left hand side of equations (1) and (2) to zero and solving for N and Fe. Solutions for nondiazotroph resource requirements under N and Fe limitation are given in equation (5) in Table 1; the asterisks indicating the equilibrium solution. A similar solution for diazotrophs is given in equation (6) in Table 1. These solutions are also represented schematically by the "zero net growth isoclines" (ZNGIs) in Figure 1a. Resource competition theory states that, at equilibrium, among species limited by resource i, the one with the lowest requirement will be the most competitive, and this species will draw the concentration of resource i down to that level. All other species with higher resource requirements will be excluded from the system in equilibrium. Since $\mu_D < \mu_P$ and $\kappa_{FeD} > \kappa_{FeP}$, and assuming that loss rates are similar for each type, we find that

Table 1. Equilibrium Solution for Equations (1)–(4)[a]

Solution		Solution Equation Number
Equilibrium Resource Requirement for Nondiazotrophs		
$Fe_P^* = \frac{\kappa_{Fe_P} m_P}{\mu_P - m_P},\ N_P^* = \frac{\kappa_{N_P} m_P}{\mu_P - m_P}$		(5)
Equilibrium Resource Requirement for Diazotrophs		
$Fe_D^* = \frac{\kappa_{Fe_D} m_D}{\mu_D - m_D}$		(6)
Phytoplankton Biomass		
$P_P^* = \frac{1}{m_P}\left(S_N^* + m_D P_D^*\right)$		(7a)
$= \frac{1}{R_P + R_D}\frac{1}{m_P}\left(S_{Fe}^* + R_D S_N^*\right)$		(7b)
$P_D^* = \frac{1}{R_P + R_D}\frac{1}{m_D}\left(S_{Fe}^* - R_P S_N^*\right)$		(8)
$P_P^* + P_D^* = \frac{1}{R_P + R_D}\left(S_N^*\left(\frac{R_D}{m_P} - \frac{R_P}{m_D}\right) + S_{Fe}^*\left(\frac{1}{m_P} + \frac{1}{m_D}\right)\right)$		(9)
$P_D^* : P_P^* = \frac{m_P}{m_D}\frac{S_{Fe}^* - R_P S_N^*}{S_{Fe}^* + R_D S_N^*}$	< 1	(10)
Resource Supply Ratio		
$S_{Fe}^* : S_N^* = R_P\left(\frac{m_P P_P^* + m_D \frac{R_D}{R_P} P_D^*}{m_P P_P^* - m_D P_D^*}\right)$	$\geq R_P$	(11)

[a]The left hand side of equations (1) through (4) are set to zero and we solve for N^*_j, Fe^*_j, and P^*_j where superscript * indicates the steady state solution and $j = P,D$.

$Fe_P^* < Fe_D^*$ (i.e. nondiazotrophs can exist at lower iron concentrations than diazotrophs, see Figure 1a). Thus, in regions where both types of phytoplankton are iron limited, nondiazotrophs will draw *Fe* down to a concentration too low for diazotrophs and these will be excluded.

[11] If the nondiazotrophs are nitrogen limited, they control the fixed nitrogen environment ($N = N_P^*$), and two situations are possible; ambient iron concentrations may be higher than the level required by nondiazotrophs, but still too low to support the higher iron requirements of diazotrophs (line A to B in Figure 1a). Alternatively there may be enough iron for the two species to coexist (point B in Figure 1a). If there is sufficient iron to support both plankton types, environmental iron will be drawn down to Fe_D^* by the diazotrophs, and environmental nitrogen will be drawn down to N_P^* by the nondiazotrophs. Thus, the two species coexist only for resource concentrations located at the intersection of the two ZNGIs.

2.2. Community Composition

[12] The equilibrium solution for the two phytoplankton types can be found by solving for P_P^* and P_D^* in equations (3) and (4), and with various substitutions provide equations (7a), (7b), (8), (9), and (10) in Table 1. There is a feedback between the two populations. Diazotrophs provide additional fixed nitrogen to the system, so their presence bolsters the nondiazotroph population (equation (7a) in Table 1). Any increase in the supply of iron or nitrogen will thus lead to an increase in nondiazotrophs and total biomass (equations (7b) and (9) in Table 1). Diazotrophs, however, only survive if there is an excess supply of iron relative to $R_P S_N^*$ (equation (8) in Table 1). Further, there will always be more nondiazotrophs than diazotrophs (equation (10) in Table 1). Since P_D^* is a function of $-S_N^*$ and P_P^* is a function of $+S_N^*$, in regions of larger absolute nitrogen supply the diazotrophs will be a smaller proportion of the biomass.

2.3. Effects of Iron Supply

[13] Consider an idealized surface ocean transect across a gradient of increasing *Fe* supply (Figure 2). Nondiazotrophs will be *Fe* limited when the *Fe* source is very low and, as discussed above, diazotrophs are excluded from such an environment. In this region where $P_D^* = 0$, under equilibrium conditions, the supply ratio, $S_{Fe}^*:S_N^*$, must balance the nondiazotroph uptake ratio, R_P (see arrows in Figure 1b). The biomass of nondiazotrophs increases in regions where iron (and nitrate) supply is higher (equation (7b) in Table 1). The $S_{Fe}:S_N$ supply ratio still must balance the nondiazotroph uptake ratio, but the local *N* concentration declines as *N* is consumed in a fixed ratio to increasing *Fe*.

[14] As the iron supply continues to rise, *N* is eventually drawn down to a point where it, rather than *Fe*, begins to limit nondiazotroph growth (dashed vertical line in Figure 2). Subsequently, as the local *Fe* concentration builds up with increasing supply, *Fe* will eventually reach Fe_D^*, the equilibrium requirement for diazotrophs (at the solid vertical line in Figure 2). This allows diazotrophs to exist alongside the population of nondiazotrophs. Further increases in the *Fe* supply support a higher concentration of both plankton types (equation (9) in Table 1): The increased *Fe* supply supports a larger population of *Fe* limited diazotrophs, and the related nitrogen-fixation supports a larger population of

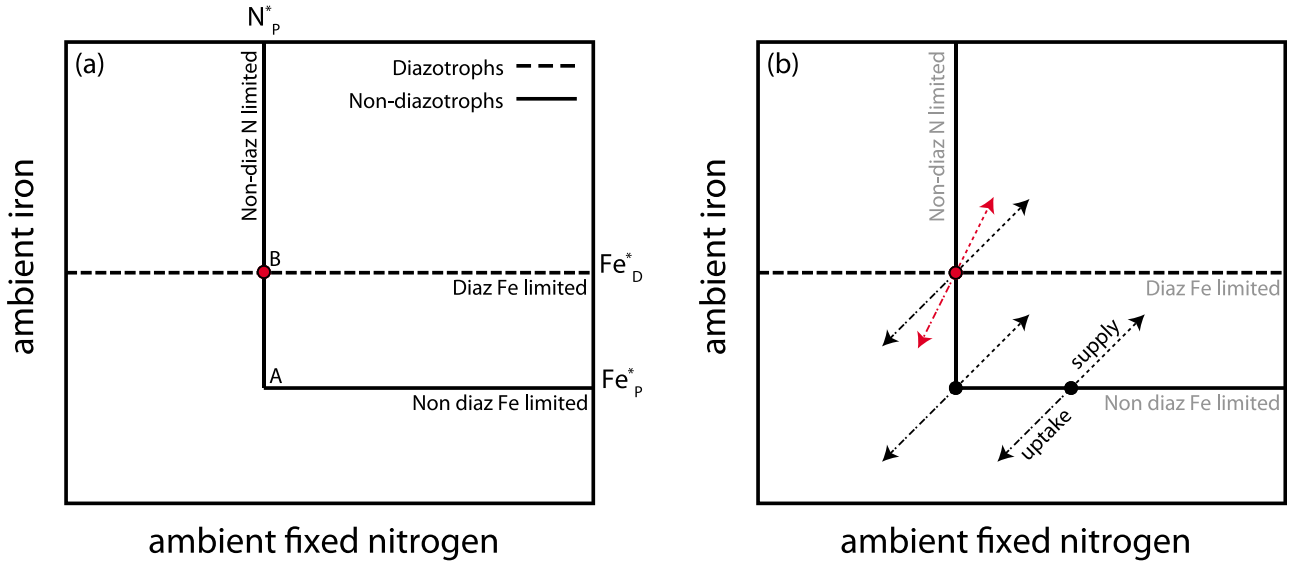

Figure 1. Theoretical framework. A schematic representation of equilibrium solutions with respect to resource concentrations represented by "zero net growth isoclines" (ZNGIs) [*Tilman*, 1982]. (a) The horizontal dashed line indicates the ZNGI for diazotrophs at $Fe = Fe^*_D$ and is independent of the fixed nitrogen concentration as we assume diazotrophs fix all the nitrogen they require. The solid lines indicate the ZNGI for nondiazotroph phytoplankton, which can be either iron limited, as indicated by the horizontal line at $Fe = Fe^*_P$, or nitrogen limited, as indicated by the vertical line at $N = N^*_P$. The transition between iron and nitrogen limitation occurs at point A. Our assumptions dictate that the iron-limited part of the ZNGI for nondiazotrophs will always lie below the ZNGI for diazotrophs. Coexistence is only possible at the intersection of the two ZNGIs (red dot at point B), where nondiazotrophs are nitrogen limited, and there is also enough iron to support diazotrophs. (b) Arrows represent resource uptake (dot-dash) and supply (dashed) vectors, with the slopes indicating the elemental supply and uptake ratios. Equilibrium requires that uptake vectors are matched by supply vectors of equal magnitude and opposite direction. The black resource vectors indicate equilibria where the ratio of uptake and supply are equal to the nondiazotroph Fe:N ratio, R_P. Where diazotrophs co-exist, their higher demand for iron increases the uptake and supply ratios (S_{Fe}:$S_N > R_P$), as indicated by the increased gradient of the red resource vectors (see equations (10) and (11) in Table 1). The higher the diazotroph biomass, the steeper the slope of the red arrows.

nondiazotrophs (equations (7a) and (7b) in Table 1). The presence of diazotrophs in the community both requires, and demands an excess of iron relative to nitrogen in the supply terms (S^*_{Fe}:$S^*_N \geq R_P$, equation (11) in Table 1). The surplus of S_{Fe} in the supply is demanded by not only the additional consumption of Fe by the diazotrophs ($m_D P_D R_D$), but also by extra nondiazotroph Fe consumption supported by newly fixed nitrogen ($m_D P_D R_P$). Thus the excess supply of Fe relative to fixed N is balanced by nitrogen fixation, together with additional consumption of both resources. As S_{Fe} increases relative to S_N (increase slope of uptake/supply of red arrow in Figure 1b), more diazotrophs are supported (equation (8) in Table 1).

2.4. Theoretical Insights

[15] In a system where autotrophic diazotrophs, limited by iron, compete with nondiazotrophic autotrophs which are limited by either inorganic nitrogen or iron we have developed the following insights:

[16] 1. Since diazotrophs are assumed to have lower maximum growth rates and higher iron requirement, they will be out-competed by other phytoplankton when iron is scarce ($Fe^*_P < Fe^*_D$).

[17] 2. In these regions where nondiazotrophic phytoplankton are iron limited, iron concentrations are controlled by physiology and mortality of the nondiazotrophs (equation (5) in Table 1).

[18] 3. Diazotrophs only exist in regions where nondiazotrophs are nitrogen limited *and* where there is excess iron supply: the source of iron relative to the source of fixed nitrogen (excluding nitrogen fixed by diazotrophs) must be greater than the ratio of cellular iron to nitrogen of nondiazotrophs (R_P, equations (8) and (11) in Table 1).

[19] 4. In regions where diazotrophs do exist, they will be iron limited (at least in the two nutrient context developed here), and iron concentrations will be controlled by the diazotrophs' physiology and mortality (equation (6) in Table 1), while nitrogen-limited nondiazotrophs will control the fixed nitrogen concentrations (equation (5) in Table 1).

[20] 5. Nondiazotroph biomass will increase with increasing biomass of diazotrophs (by, for instance, an increased external supply of iron) as additional fixed nitrogen is added to the system (equation (7a) in Table 1).

[21] 6. Though they can co-exist with other phytoplankton, diazotrophs will never dominate the biomass (equation (10) in Table 1).

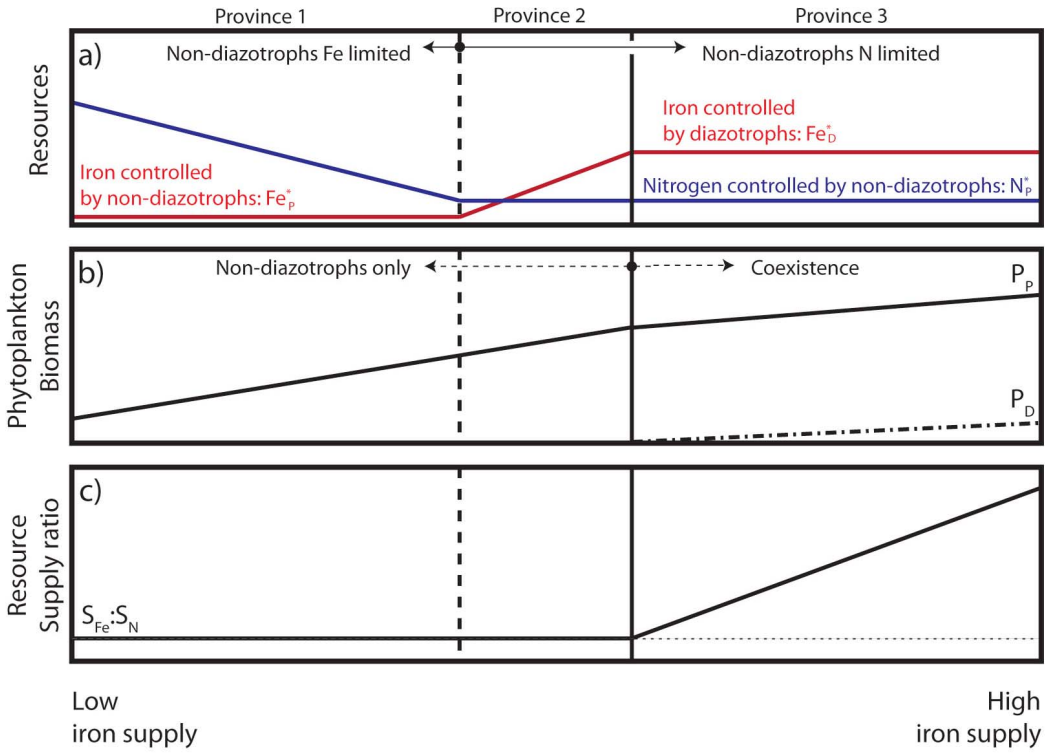

Figure 2. Theoretical framework. Schematic diagram representing a surface transect from low to high iron supply. S_N is assumed to increase in fixed ratio to S_{Fe} up to the solid vertical line and then remain uniform across the remainder of the transect. (a) Nutrient concentrations (red = iron; blue = fixed nitrogen); (b) phytoplankton biomass (solid line = nondiazotroph; dashed line = diazotroph); (c) ratio of iron to nitrogen supply (solid line), dashed line indicated R_P (the nondiazotroph *Fe*:*N* uptake ratio). We find three distinct provinces, separated by the vertical lines (see text).

[22] The delineation between co-existence and exclusion of two phytoplankton types with different requirements for two nutrients discussed here mirrors that found in work by *Tilman* [1977]. We now demonstrate the applicability and usefulness of this framework in interpreting the results from a complex numerical ecosystem model, focusing on the iron and fixed nitrogen limited Pacific Ocean.

3. Model Description

[23] We briefly describe the three-dimensional ocean model and some basic features of its biogeography. The model has been discussed previously by *Follows et al.* [2007], *Dutkiewicz et al.* [2009], and *Monteiro et al.* [2010]. It is based on a coarse resolution (1° × 1° horizontally, 24 levels) configuration of the MIT general circulation model (MITgcm) [*Marshall et al.*, 1997] constrained to be consistent with altimetric and hydrographic observations (the ECCO-GODAE state estimates [*Wunsch and Heimbach*, 2007]). We transport inorganic and organic forms of nitrogen, phosphorus, iron and silica, and resolve several phytoplankton types as well as two simple grazers. The biogeochemical and biological tracers interact through the formation, transformation and remineralization of organic matter. Excretion and mortality transfer living organic material into sinking particulate and dissolved organic detritus which are respired back to inorganic form. The time dependent change in the biomass of each of the model phytoplankton types, P_j, is described in terms of growth, sinking, grazing, other mortality and transport by the fluid flow. Phytoplankton growth is function of light, temperature and nutrient resource as described in Appendix B and *Dutkiewicz et al.* [2009]. Tables 2 and 3 provide the specific parameters used in these experiments, symbols and equations not described here can be found in work by *Dutkiewicz et al.* [2009].

[24] Iron chemistry includes explicit complexation with an organic ligand, and scavenging by particles [*Parekh et al.*, 2005]. We have modified the iron model relative to *Dutkiewicz et al.* [2009] and *Monteiro et al.* [2010] in three ways (details in Appendix B): 1) we parameterize the scavenging as a function of the concentration of particulate organic carbon (POC); 2) we parameterize a sedimentary source (F_{sed}) as a function of the sinking organic matter reaching the ocean bottom as suggested by the measurements of *Elrod et al.* [2004]; 3) the Aeolian source includes a regional estimate of the soluble fraction [*Luo et al.*, 2008]. These modifications improved iron fields in the model relative to work by *Dutkiewicz et al.* [2009] and *Monteiro et al.* [2010, 2011], in particular, increased iron in the south subtropical gyre in the Pacific Ocean.

[25] We resolve six candidate phytoplankton functional types that are representative of the marine community with many types in work by *Dutkiewicz et al.* [2009] and *Monteiro et al.* [2010]. We resolve a diatom, a large non-diatom phytoplankton, high and low light *Prochloroccus*, a

Table 2. Ecosystem Model Parameters That Vary Between Phytoplankton Types[a]

Parameter	Symbol	Diatom[b]	Large[c]	Proch[d]	Small[e]	Trich[f]	Unicell[g]	Units
phyto max growth rate at 30°C	$\mu_{\max}$	2.5	2.5	1.4	1.4	1.25	0.70	d^{-1}
phyto elemental ratios	$R_{Si:P}$	16	–	–	–	–	–	
	$R_{N:P}$	16	16	16	16	40	40	
	$R_{Fe:P}$	$1*10^{-3}$	$1*10^{-3}$	$1*10^{-3}$	$1*10^{-3}$	$3*10^{-2}$	$3*10^{-2}$	
	$R_{Fe:N}$	$6.25*10^{-5}$	$6.25*10^{-5}$	$6.25*10^{-5}$	$6.25*10^{-5}$	$7.5*10^{-4}$	$7.5*10^{-4}$	
growth half saturation coefficients	κ_{PO4}	$3.5*10^{-2}$	$3.5*10^{-2}$	$1.0*10^{-2}$	$1.5*10^{-2}$	$3.5*10^{-2}$	$1.5*10^{-2}$	μ M P
	κ_{NO3}	0.56	0.56	–	0.24	–	–	μM N
	κ_{NH4}	0.28	0.28	0.08	0.12	–	–	μM N
	κ_{Fe}	$3.5*10^{-5}$	$3.5*10^{-5}$	$1.0*10^{-5}$	$1.5*10^{-5}$	$1.1*10^{-3}$	$3.6*10^{-4}$	μM Fe
	κ_{Si}	0.56	–	–	–	–	–	μM Si
PAR inhibition coefficient	k_{inhib}	$1*10^{-3}$	$1*10^{-3}$	HL[h]: $3*10^{-3}$ LL[h]: $6*10^{-3}$	$3*10^{-3}$	$1*10^{-3}$	$3*10^{-3}$	
phyto sinking rate	w^P	0.5	0.5	0.0	0.0	0.5	0.0	m d^{-1}
phyto palatability	η	0.85	0.9	1.0	1.0	0.9	1.0	
DOM/POM partitioning	λ_{mp}	0.3	0.3	0.05	0.05	0.3	0.05	
	λ_g	0.6	0.6	0.3	0.3	0.6	0.3	

[a]See *Dutkiewicz et al.* [2009, appendix] for equations.
[b]"Diatom" refers to large phytoplankton that require silica (diatom-analogs).
[c]"Large" refers to large phytoplankton that do not require silica.
[d]"Proch" refers to *Prochloroccus*-analogs.
[e]"Small" refers to small phytoplankton that require nitrate.
[f]"Trich" refers to *Trichodesmium*-analogs.
[g]"Unicell" refers to unicellular diazotroph-analogs.
[h]"HL" and "LL" refer to high and low light *Prochloroccus*-analogs.

Table 3. Ecosystem Model Parameters That Are Fixed for All Simulations[a]

Parameter	Symbol	Fixed Value	Units
temperature coefficients	A_E	−4000	K
	T_o	293.15	K
phytoplankton mortality	m^P	0.1	d^{-1}
ammonium inhibition	ψ	4.6	$(\mu M\ N)^{-1}$
maximum grazing rate at 30°C	$g_{\max_a}$	0.625	d^{-1}
	$g_{\max_b}$	0.179	d^{-1}
grazing half saturation	κ^P	0.085	μM P
zooplankton mortality	m^Z	0.033	d^{-1}
DOM/POM partitioning	λ_{mpl}	0.6	
	λ_{mps}	0.3	
DOM remineralization rate at 30°C	r_{DOP}	0.02	d^{-1}
	r_{DON}	0.02	d^{-1}
	r_{DOFe}	0.02	d^{-1}
POM remineralization rate at 30°C	r_{POP}	0.04	d^{-1}
	r_{PON}	0.04	d^{-1}
	r_{POFe}	0.04	d^{-1}
	r_{POSi}	0.0067	d^{-1}
POM sinking rate	w_{POM}	10	m d^{-1}
POC:POP	$R_{C:P}$	106	
NH_4 to NO_2 oxidation rate	ζ_{NO2}	2	d^{-1}
NO_2 to NO_3 oxidation rate	ζ_{NH4}	0.1	d^{-1}
critical PAR for oxidation	I_{ox}	10	μEin m^{-2} s^{-1}
ligand binding strength	β_{Fe}	$2*10^5$	$(\mu M)^{-1}$
total ligand	L_T	$1*10^{-3}$	μM
scavenging rate coefficient	c_o	$1.2*10^{-3}$	d^{-1}
scavenging power coefficient	ϕ	0. 58	
sedimentation rate ratio	R_{sed}	$6.4 * 10^{-5}$	μM Fe/d$(\mu$M POP/d$)^{-1}$
PAR attenuation coefficients	k_o	0.04	m^{-1}
	k_P	0.64	$(\mu$M P$)^{-1}$ m^{-1}

[a]See *Dutkiewicz et al.* [2009, appendix] and Appendix B for equations.

Table 4. List of Simulations

Experiment Name	Diazotroph Types	Iron Source	Half Saturation	Nitrogen Fixation[a]	Primary Production[a]
Control	generic diaz[b]	modern[c]	κ_{FeP}, κ_{FeD}[d]	45.4 (85.3)	14.3 (37.9)
K_{Fe}Phyto	generic diaz	modern	$\frac{1}{2}\kappa_{FeP}$, κ_{FeD}	45.5 (85.4)	14.3 (38.4)
K_{Fe}Diaz	generic diaz	modern	κ_{FeP}, $\frac{1}{2}\kappa_{FeD}$	56.1 (97.2)	14.6 (38.2)
LoIron	generic diaz	$\frac{1}{2}\times$ modern	κ_{FeP}, κ_{FeD}	34.0 (71.4)	13.8 (37.1)
NoDiaz	none	modern	κ_{FeP}	0 (0)	12.7 (34.8)
NoDiazLoIron	none	$\frac{1}{2}\times$ modern	κ_{FeP}	0 (0)	12.5 (34.5)
MultDiaz	Trich and Unicell[e]	modern	κ_{FeP}, κ_{FeD}	52.2 (91.0)	14.6 (38.3)
MultDiazLoIron	Trich and Unicell	$\frac{1}{2}\times$ modern	κ_{FeP}, κ_{FeD}	38.1 (75.6)	14.0 (37.4)
DiazHiIron	generic diaz	4× modern	κ_{FeP}, κ_{FeD}	92.9 (135.5)	15.9 (40.5)
DiazPreIron	generic diaz	preindust.[c]	κ_{FeP}, κ_{FeD}	34.5 (66.5)	13.9 (37.1)

[a]Nitrogen fixation rates are in TgN/y and primary production is in GtC/y. The first number is rate for Pacific ocean from 45°S to 45°N, number in parentheses is the global rate.
[b]"Generic diaz" refers to a generic diazotroph type.
[c]The terms "modern" and "preindust" refers to the modern and pre-industrial dust flux as modeled by *Luo et al.* [2008].
[d]"κ_{FeP}, κ_{FeD}" refer to the half saturation of growth of the nondiazotrophs and diazotrophs respectively and $\frac{1}{2}$ refers to a halving of the values as given in Table 2.
[e]"Trich" refers to *Trichodesmium*-analogs; "Unicell" refers to unicellular diazotroph-analogs.

small nitrate using phytoplankton and a diazotroph. Here for simplicity we consider only a single generic diazotroph type, but in additional simulations (discussed in Appendix C) we differentiate between two diazotrophs (*Trichodesmium* and a unicellular diazotroph type) following *Monteiro et al.* [2010]. Diazotrophs are parameterized as described by *Monteiro et al.* [2010] with a lower maximum growth rate (energetic expense of breaking the nitrogen triple bond) and requiring more iron (additional iron needed for the nitrogenase enzyme). For simplicity, diazotrophs are assumed to fix all the nitrogen they require. A crude parameterization of denitrification as by *Monteiro et al.* [2010] is imposed: nitrate below 200 m is modified so that nitrate:phosphate ratios are restored to observed values [*Garcia et al.*, 2006] only if there is excess nitrate. Over the short integration times in these experiments, this formulation provides the necessary sink of nitrogen.

[26] The model is sufficiently complex to reflect relevant properties of marine phytoplankton communities and natural interactions, and can serve as an ecological "laboratory" in which to explore the relevance of theoretical concepts of community structure and ecosystem-iron-nitrogen cycle interactions. Thus we will seek to interpret the regulation of community structure and iron concentrations in the model using the framework laid out in section 2.

[27] We first show results from a "control" simulation (Control) and then compare to those from several sensitivity experiments (Table 4) to illustrate the biological control of iron in the model ocean (experiments K_{Fe}Phyto and K_{Fe}Diaz) and to explain how nutrients and phytoplankton communities respond to changes in the supply of iron (experiment LoIron). Results from additional experiments are shown in Table 4 and are described briefly in Appendix C. All simulations were integrated for 10 years, initialized with nutrient and organic fields from a previous simulation (precise details of the initial fields do not impact the results presented here). In the following we examine and compare the annual average results from the 10th year.

4. Control Simulation (Control)

[28] The model global primary production is 38 GtC/y which is on the low end of satellite derived estimates of primary production (35–52 GtC/y [e.g., *Behrenfeld and Falkowski*, 1997; *Uitz et al.*, 2010; *Westberry et al.*, 2008]), however the highly productive coastal regions are not captured at such low resolution. In this control run the global nitrogen fixation is 85 TgN/y which compares favorably to the range 55 to 135 suggested by other recent studies [*Capone et al.*, 1997; *Gruber*, 2004; *Deutsch et al.*, 2007; *Moore et al.*, 2004]. The model (similar to those described by *Dutkiewicz et al.* [2009], *Monteiro et al.* [2010, 2011], and *Saba et al.* [2010]) captures the observed high biomass, high macro-nutrient subpolar and equatorial regions as well as the low biomass, low macro-nutrient subtropical gyres. The anticipated high nutrient, low Chlorophyll regions of the Southern Ocean, Northern Pacific and Equatorial Pacific are also captured. Distribution of nondiazotrophic phytoplankton types are similar to those described by *Dutkiewicz et al.* [2009] and the distribution of autotrophic diazotroph biomass and nitrogen fixation rates are similar to those described by *Monteiro et al.* [2010], which were in accord with (sparse) observations. In the following we will consider all nondiazotrophic phytoplankton aggregated together (and refer to these as "nondiazotrophs"), though note that there is a more complex pattern with regard to which of these types coexist and out compete each other in different areas [see *Dutkiewicz et al.*, 2009].

[29] Nondiazotroph's growth can be limited by the availability of iron, fixed nitrogen (nitrate, nitrite and ammonium) and phosphorus. Over most of the model ocean the former two are most relevant, though there are small regions of the Atlantic and Indian Ocean where phosphorus limitation is important. For the rest of this study, where we apply the simple two nutrient framework of section 2, we therefore concentrate on the Pacific Ocean. As shown by *Dutkiewicz et al.* [2009], in regions where the mixed layer depth varies annually by less than about 250 m, the annual average results can be considered close to equilibrium and the steady state resource competition theory is applicable. Only low latitude regions fall into this category, thus we additionally limit our study to the Pacific equatorward of 45°. Since diazotrophs have a low maximum growth rate they are out competed in transient blooms and are excluded from higher latitudes anyway [*Monteiro et al.*, 2011].

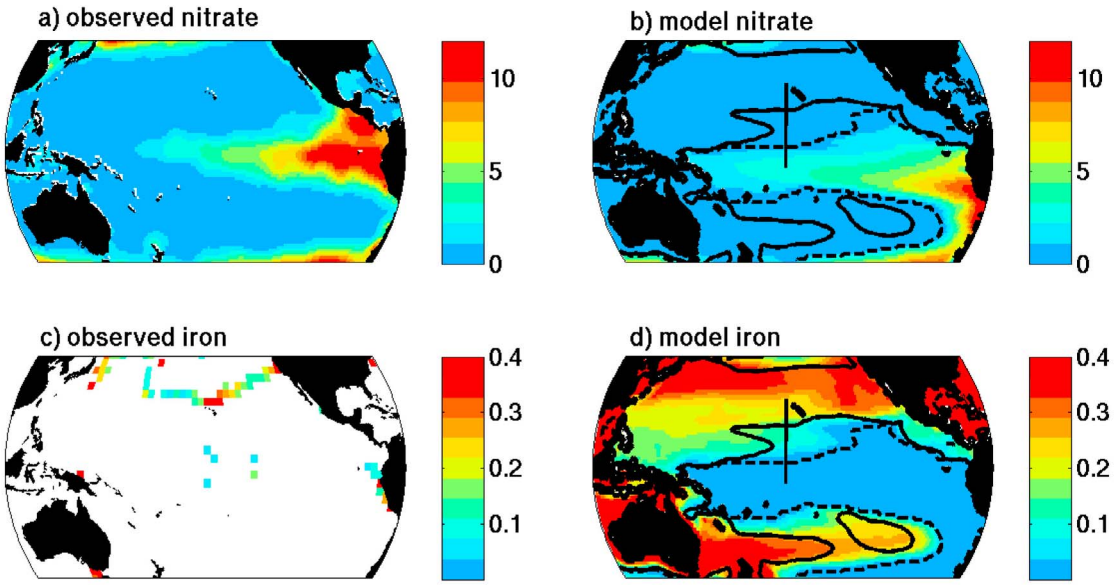

Figure 3. Observations and control simulation. Annual mean (0–50 m): (a) Observed nitrate (μM N) from World Ocean Atlas [*Garcia et al.*, 2006]; (b) model fixed nitrogen (μM N), which includes nitrate, nitrite and ammonium; (c) observed iron (nM Fe) from compilation of *Moore and Braucher* [2008], since data are not from all months this does not represent a true annual mean; (d) Model iron (nM Fe). In Figures 3b and 3d the dashed line indicates separation of regions that are iron or fixed nitrogen limited (see Figure 4c) in the model. Solid line indicates region where model diazotroph concentration are above 10^{-5} μ M N (see Figure 4b). Location of transect shown in Figure 5 is also indicated.

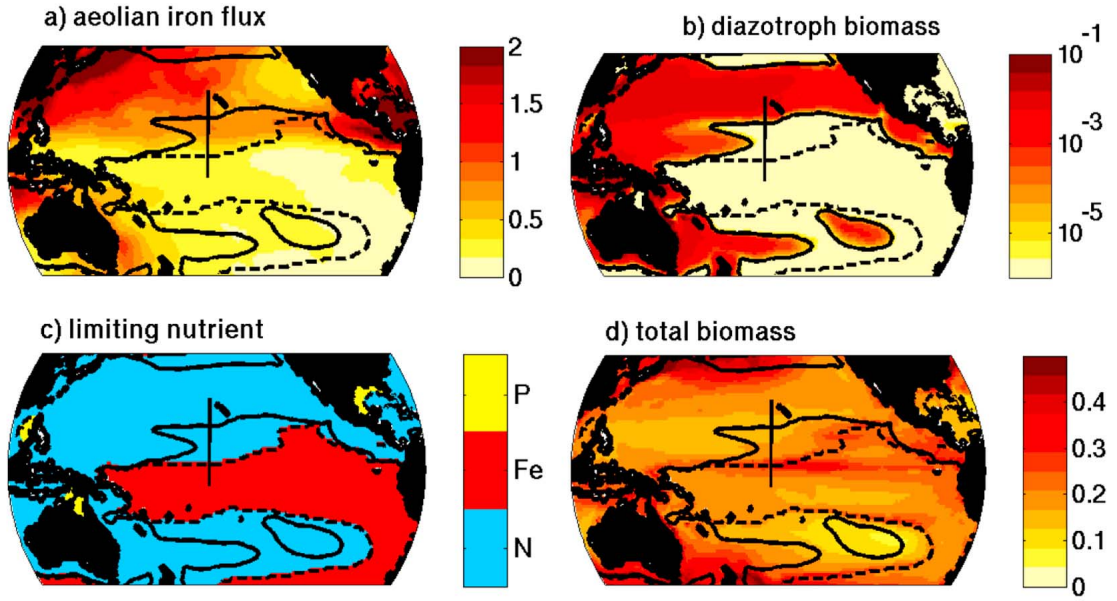

Figure 4. Control simulation. Annual mean: (a) Bio-available aeolian iron flux (10^{-5} mmol/m^2/y, from *Luo et al.* [2008]); (b) diazotroph biomass averaged over 0–50 m (μM N, log shading); (c) nutrient limiting nondiazotroph phytoplankton growth (red = iron, blue = fixed nitrogen, yellow = phosphate); (d) total phytoplankton biomass averaged over 0–50 m (μM N). Dashed line indicates separation of regions that are iron or fixed nitrogen limited (as shown in Figure 4c). Solid line indicates region where diazotroph concentration are above 10^{-5} μ M N (as shown in Figure 4b). Location of transect shown in Figure 5 is also indicated.

[30] Similar to observations [e.g., *Garcia et al.*, 2006], modeled nitrate is low over much of the low latitude Pacific, with higher concentrations from upwelling along the equator (Figures 3a and 3b). Modeled iron is very low over much of the equatorial regions and higher in the northern Pacific and the western southern subtropical gyre (Figure 3d), largely mirroring the aeolian dust source (Figure 4a), though enhanced especially in the western subtropical gyre by sedimentary sources. Observations of iron are sparse (Figure 3c) especially in the southern Pacific, but do suggest a gradient from higher iron in the northern Pacific to lower in the equatorial regions.

[31] Though the numerical model is more complex than the simple framework discussed above (e.g. effects of light and temperature on growth, explicit grazing), it mirrors the qualitative understanding of the distribution of diazotrophs (Figure 4b). As anticipated in section 2, diazotrophs do not exist where the nondiazotrophs are iron limited (dashed line in Figure 4, red area in Figure 4c), but not all regions where nondiazotrophs are nitrogen limited support diazotrophs. Diazotrophs occupy regions of higher iron that are similar to those seen in work by *Monteiro et al.* [2010], except in some parts of the southern subtropical gyre where higher iron concentration in this current study allow higher concentration of diazotrophs. *Monteiro et al.* [2010] showed that the patterns and concentrations of diazotrophs are consistent with the sparse observations. In particular the lack of diazotrophs in the Pacific equatorial and eastern subtropical gyre is in agreement with cruises that specifically did not detect diazotrophs in those regions [*Church et al.*, 2008; *Mague et al.*, 1974; *Bonnet et al.*, 2008]. Where they do exist, diazotrophs contribute only a small percentage (in general less the 1%, but up to as much as 5%) to the local biomass (this result is also anticipated by the framework, equation (10) in Table 1). However by adding new fixed nitrogen to the system diazotrophs are directly and indirectly responsible for as much as 8% of the global primary production, though this should be seen as an upper bound (see discussion of experiment NoDiaz in Appendix C).

[32] Figure 5 shows a surface transect (position indicated in Figures 3 and 4) which passes through distinctly different regions and with steadily increasing aeolian supply of iron northward (Figure 4a). The source of iron is a combination of aeolian, sedimentary, horizontal and vertical transport, mixing, as well as remineralization of organic iron. The source of fixed nitrogen to the euphotic layer (as assumed here) does not include an external source and only includes horizontal and vertical transport, mixing, and remineralization of organic matter. This facilitates a disconnect in the supply ratio to the north where Aeolian iron inputs are large. Complexities of the numerical model relative to the simple framework (e.g. temperature and light dependent growth rates) result in a figure that is more complicated than its theoretical analogue (Figure 2). However, the three different provinces suggested by the framework of section 2 are present:

[33] 1. To the south where iron supply is low, diazotrophs are excluded, concentrations of fixed nitrogen are high, nondiazotrophs are iron limited, and iron concentrations are low. The iron to nitrogen supply ratios adjust (see discussion below and work by *Tilman* [1982]) to remain near or at R_P (the cellular iron-to-nitrogen ratio of the nondiazotrophs).

[34] 2. In a transition province nondiazotrophs become nitrogen limited, but diazotrophs are still excluded. Here iron concentrations increase, nitrogen is low and, iron to nitrogen supply ratios are still near or at R_P.

[35] 3. To the north where iron supplies are higher, diazotrophs and nondiazotrophs co-exist. Iron to nitrogen supply ratios are much greater than R_P, nitrogen concentrations remain low, and iron concentrations are higher than in any other parts of the transect.

[36] In the first two regions, iron to nitrogen supply ratios adjust to remain near or at R_P; any excess of one or the other nutrient relative to this ratio leads to local accumulation, and hence a reduction in the gradient of that nutrient. There is a consequent reduction in the supply of that nutrient until the ratio of supply equilibrates at R_P. This quasi-steady state is reached in only a couple of years of integration (though we note that long term drifts as deep water reaches the surface will continue for many thousands of years, but the qualitative results from these simulations do not change with length of simulation after the first few years adjustment).

[37] In the first, iron limited, region, increases in the aeolian iron flux northward lead to elevated nondiazotroph biomass with increased drawdown of excess nitrogen (relative to R_P). Moving into region 2, the iron flux becomes sufficient to allow the consumption of all excess nitrogen, and the nondiazotrophs become nitrogen limited for the first time. Excess iron, relative to R_P, now accumulates to the north, and will eventually reach a level at which diazotrophs are able to invade. Northward of this point, in region 3, iron and nitrogen uptake are decoupled as diazotrophs and nondiazotrophs coexist, and hence the supply ratio is able to deviate from R_P.

[38] From the theoretical framework of section 2, we anticipate that the concentrations of iron and fixed nitrogen are controlled by either diazotrophs or nondiazotrophs in the different provinces. Since growth rates and half saturation constants are not fixed as in the theoretical framework, this is not as easy to gauge in Figure 5. The nutrient concentrations at equilibrium, N_P^*, Fe_j^* can be calculated numerically. However these values now include additional non-linear terms such as grazing and sinking, and we found that sensitivity studies were much clearer in elucidating the control of the phytoplankton on their nutrient environment [see *Dutkiewicz et al.*, 2009].

5. Sensitivity Experiments

5.1. Biological Control of Iron in the Pacific

[39] The simplified framework of section 2 suggests that iron concentrations will be controlled by nondiazotrophs in regions where they are iron limited (Table 1, equation (5)), while in regions where diazotrophs are iron-limited, iron concentrations should be set by diazotroph physiology and loss rates, as given in equation (6) in Table 1. Here we conduct two sensitivity simulations, where we manipulate the physiology of the phytoplankton (specifically through the iron half saturation, K_{Fej}) to illustrate that they do indeed control iron concentrations.

5.1.1. Changing Physiology of Nondiazotrophs (K_{Fe}Phyto)

[40] In this experiment κ_{Fe_p} of all nondiazotrophic phytoplankton types was half that used in the Control simulation. The ambient concentrations of iron were half of the Control simulation (Figure 6a) in the regions where the nondiazotrophs

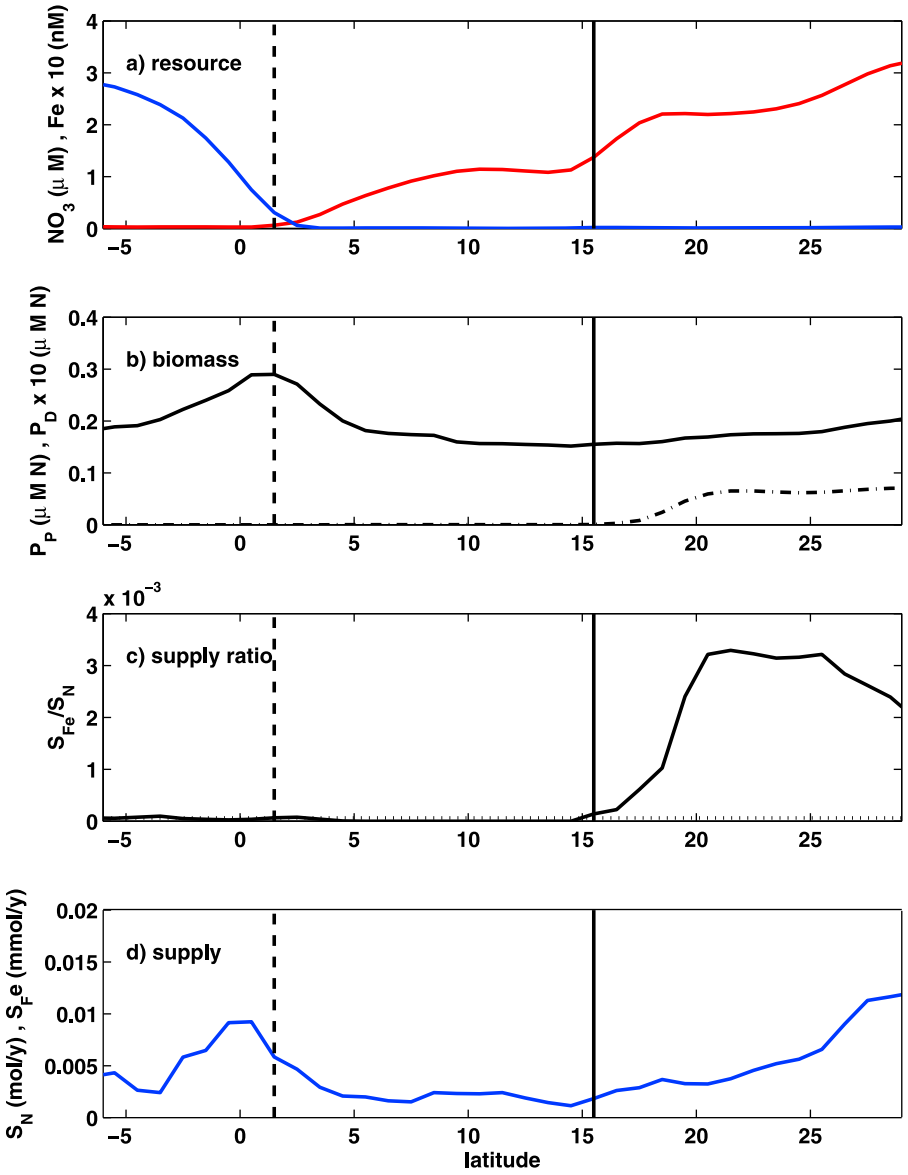

Figure 5. Control simulation. Transect (0–50 m average) indicated in Figure 4 (compare to theoretical analog, Figure 2). (a) Nutrient concentrations (red = 10 × iron, nM; blue = fixed nitrogen, μM); (b) phytoplankton biomass in nitrogen currency, μM N (solid = nondiazotroph; dashed = 10 × diazotroph); (c) ratio of iron to nitrogen supply, dotted line indicated R_P; (d) nutrient supply (red = iron, nM/s; blue = fixed nitrogen, μM/s). Nutrient sources include aeolian and sedimentary (iron only), lateral, vertical supply and source from remineralization of organic matter. Vertical dashed lines indicate the transition from iron to fixed nitrogen limitation for nondiazotrophs. Vertical solid lines indicate transition from no diazotroph to co-existence with the nondiazotrophs. Iron is not constant to the right of vertical solid line (as in Figure 2) as Fe_D^* is a function of temperature and light which change along this transect. Similarly, nondiazotroph biomass, P_P^*, is also a function of the fixed nitrogen source in the numerical simulation, which changes over the transect (see, for instance, increase at equator).

were iron limited (red regions of Figure 4c). Elsewhere the iron concentrations remained the same. This suggests nondiazotroph physiology does control the annual averaged iron concentrations in iron-limited regions (equation (5) in Table 1) of the model Pacific Ocean.

5.1.2. Changing Physiology of Diazotrophs (K_{Fe}Diaz)

[41] If now we halve κ_{Fe_D} instead, we find the opposite pattern with iron concentrations half of the Control simulation (Figure 6b) in much of the regions where nondiazotrophs are limited by fixed nitrogen (blue areas of Figure 4c). Here Fe_D^* is half that in the Control simulation and, as anticipated in section 2 diazotroph physiology does indeed control the annual averaged iron concentrations in regions where they are iron-limited (equation (6) in Table 1). Because Fe_D^* is smaller in this experiment, a lower iron source can maintain these values and we find that more regions can support diazotrophs (Figure 7c) leading to a 14% global increase in nitrogen fixation (Table 4).

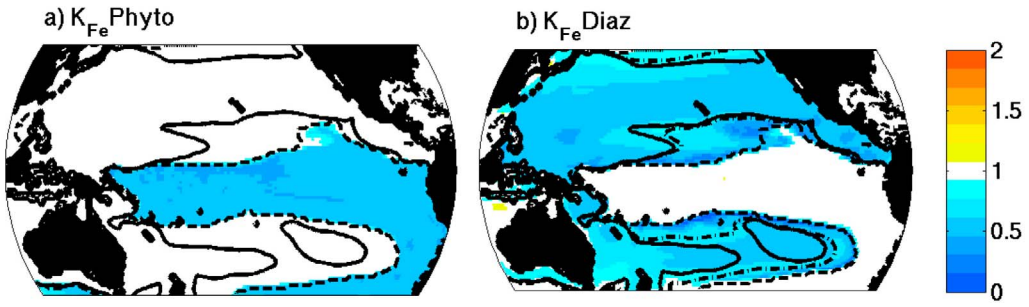

Figure 6. Ratio of sensitivity experiments to control simulation. Annual mean (0–50 m) iron concentration from sensitivity experiment divided by that from Control simulation: (a) K_{Fe}Phyto experiment where iron half saturation κ_{Fe_j} of all nondiazotrophs is halved relative to Control; (b) K_{Fe}Diaz where iron half saturation κ_{Fe_j} of diazotrophs is halved. Value of 1 indicates no difference between the two simulations, 0.5 indicates that iron concentrations in sensitivity experiment are half that in the control. Solid line indicates where diazotroph concentration is above 10^{-5} μM N in Control, and dashed line indicates where there is a shift from iron to fixed nitrogen limitation in Control. In Figure 6b we also indicated where diazotroph concentration is above 10^{-5} μM N in K_{Fe}Diaz experiment (dash-dotted line).

5.2. Impact of Changing Iron Supply (LoIron)

[42] In this experiment we halve the aeolian source of iron and examine the changes to nutrients and ecosystem structure. The total iron source is not halved as it also includes lateral, vertical, sediment supplies as well as remineralization of organic iron. Our comparison here will therefore consider only the sign of the changes to the system relative to the control simulation (Figure 8).

[43] A decrease in iron supply, S_{Fe} shrinks the regions able to support diazotrophs (Figure 7d) and nitrogen fixation drops 10% globally (to 71 TgN/y) with an accompanying decline in global primary production (by 1 GtC/y, see Table 4). Equation (9) in Table 1 suggests that a reduced iron supply (S_{Fe}) should lead to a reduction of total phytoplankton biomass. We find that this is true in our numerical model over much of the Pacific except in some key transition zones (Figure 8a). This exception is a result of the three-dimensional nature of the numerical model and is explained in section 6.

[44] In the equatorial Pacific where nondiazotrophs are iron limited, ambient iron concentrations do not change relative to the control (Figure 8). This result can be explained by examining equation (5) in Table 1 which suggests that here iron is independent of S^*_{Fe}. Additionally in regions where

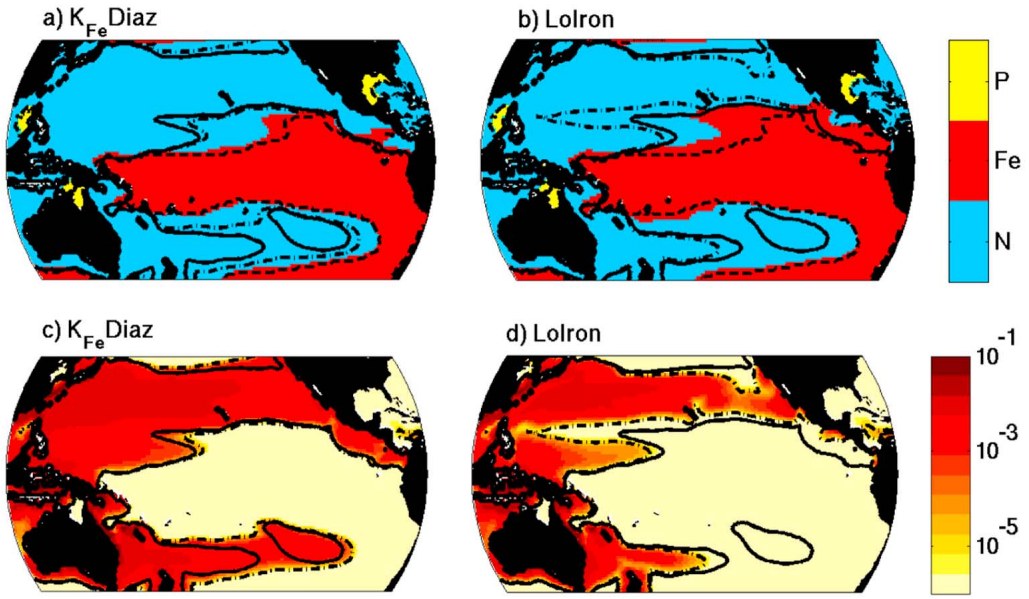

Figure 7. Sensitivity experiments. Annual 0–50 m mean: (a, b) Nondiazotroph nutrient limitation and (c, d) total diazotroph biomass (μM N). Figures 7a and 7c show K_{Fe}Diaz, experiment with half diazotroph κ_{FeD}; Figures 7b and 7d show LoIron, experiment with half aeolian iron supply. For nutrient limitation, red indicates the majority of biomass is iron limited, blue for nitrogen, yellow for phosphorus. Solid line indicates region where diazotroph concentration are above 10^{-5} μM N for Control experiment, while dash-dotted indicates the same for these sensitivity experiments. In Figures 7a and 7b the dashed line indicates separation of regions that are iron or fixed nitrogen limitation in Control.

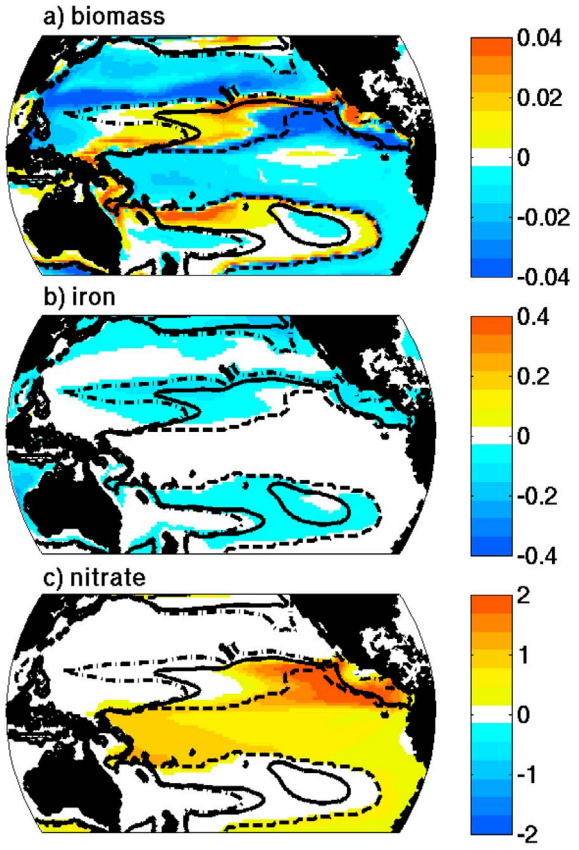

Figure 8. Difference LoIron-Control. LoIron has half aeolian supply of iron than Control. Difference between LoIron and Control for annual mean (0–50 m:) (a) Total phytoplankton biomass (μM N), (b) iron (nM Fe), (c) nitrate (μM N). Solid line indicates region where diazotroph concentration are above 10^{-5} μM N for Control, dash-dotted line indicates the same for LoIron. Dashed line indicates separation of regions with iron or fixed nitrogen limitation in Control.

diazotrophs exist, iron concentrations remain the same as the control as suggested by equation (6) in Table 1 which is also independent of S^*_{Fe}. In the transition zone iron concentrations do change between simulations (explained in section 6). Fixed nitrogen concentrations only change relative to the Control in the equatorial region (Figure 8d) where nondiazotrophs are iron limited and there is no explicit biological control on nitrogen.

6. Biogeochemical Provinces

[45] We collate the findings from the theoretical framework and the numerical model simulations to fully describe the three distinct biogeographic provinces in the low seasonality Pacific (nominally equatorward of 45 degrees). These provinces are most clearly viewed on the transect (Figure 5), but are also denoted by the contours indicating shift between fixed nitrogen and iron limitation for nondiazotrophs and the contour denoting existence of diazotrophs in Figures 4 and 7.

[46] 1. Low Iron Supply: In this province phytoplankton are iron limited and nondiazotrophic phytoplankton, which require less iron per unit nitrogen, draw the iron concentrations down to Fe^*_P which is too low to support diazotrophs. Nitrate is not limiting so concentrations are not under biological control and are free to vary with changing supply and/or demand. Here iron and nitrogen supplies are in balance with the cellular iron to nitrogen uptake ratios of the nondiazotrophs, R_P. ($Fe = Fe^*_P$, N no analytical solution, $P_P = \frac{S_N}{m_P}$, $P_D = 0$).

[47] 2. Transition: In this province iron supplies are higher, relieving the iron stress of the nondiazotrophic phytoplankton, which are instead limited by fixed nitrogen. However the iron supply is still too low to maintain the minimum iron concentration needed by diazotrophs (Fe^*_D) and diazotrophs are excluded. Here inorganic nitrogen concentrations are dictated by the dominant nondiazotrophs and, although iron concentrations are not under direct biological control, they will lie between Fe^*_P and Fe^*_D. ($Fe^*_P < Fe < Fe^*_D$, $N = N^*_P$, $P_P = \frac{S_N}{m_P}$, $P_D = 0$).

[48] 3. High Iron Supply: In this third province iron supplies are high enough to support diazotrophs, which coexist with other phytoplankton. Diazotrophs control the iron concentrations, drawing it down to Fe^*_D. Fixed nitrogen concentrations are controlled by the type of nondiazotrophs inhabiting the province. The presence of diazotrophs in the community both requires and causes an excess of iron relative to nitrogen in the supply terms (S_{Fe}:$S_N \geq R_P$ in equation (11) in Table 1). ($Fe = Fe^*_D$, $N = N^*_P$, P_P and P_D given as in equations (7a), (7b), and (8) in Table 1.)

[49] Though these results have been described by just two groups of phytoplankton, nondiazotrophs and diazotrophs, the numerical simulations did include several different types of nondiazotrophs and, in the case of Experiment MultDiaz (discussed in Appendix C) two types of diazotrophs. To maintain a succinct manuscript we have not developed this aspect of the model here. However, we do note that the provinces described above can be further divided by the type of nondiazotrophic phytoplankton that dominates [see *Dutkiewicz et al.*, 2009] or which diazotroph dominates the nitrogen fixation [see *Monteiro et al.*, 2010] and further experiment MultDiaz in Appendix C).

[50] The boundaries between the three provinces shift with changes in the external supply of iron (Figure 8) and the phytoplankton biomass, iron and fixed nitrogen concentrations respond differently within each of these provinces. Similar regional patterns of productivity change have been seen in previous modeling studies examining the effect of changes in aeolian dust [e.g., *Krishnamurthy et al.*, 2009], though they have not been explicitly explained. Following our province description above, we can now interpret the patterns seen with decreasing aeolian iron supply (Figure 8):

[51] 1. Where the limiting nutrient of the dominant, nondiazotrophic phytoplankton is iron (Province 1), biomass decreases with decreasing iron supply, but ambient iron concentrations remain fairly constant, set at Fe^*_P.

[52] 2. Decreased phytoplankton growth in Province 1 leads to local accumulation of N and hence an increase lateral supply of nitrogen to surrounding regions (the transition Province). This results in an increase in biomass downstream, with a subsequent reduction in iron in these regions. This latter result was not anticipated by the simple implications of

resource control theory, but requires the more complex three dimensional model.

[53] 3. Decreased iron supply reduces the extent of the regions where diazotrophs can exist (Province 3). Locally reduced diazotroph populations leads to reduced supply of newly fixed nitrogen which also lowers the biomass of nondiazotrophs.

[54] 4. Decreased iron supply will change the phytoplankton biomass, but as long as the types of phytoplankton that dominate in the low and high iron source provinces remain the same, the iron concentrations there will not change. This is not true in the transition province where iron concentrations are not explicitly biologically controlled.

7. Summary and Discussion

[55] Field studies have indicated the importance of nitrogen and iron concentrations with regard to the distribution of diazotrophs in the world's ocean. *Church et al.* [2008] found increased abundance of nitrogenase reductase genes (markers of diazotrophy) with decreasing nitrate concentrations along several cruise tracks in the Pacific and *Moore et al.* [2009] found a correlation between diazotrophy and iron concentrations in the Atlantic. Though these are suggestive of the strong nutrient control on diazotrophy, there has not yet been a comprehensive, mechanistic explanation of these controls. Several numerical simulations [e.g., *Moore et al.*, 2006; *Tagliabue et al.*, 2009; *Krishnamurthy et al.*, 2009] have manipulated key model parameters and iron sources and observed the global changes to nitrogen fixations rates, but have not described in detail the underlying feedback between diazotroph communities and their nutrient environments. The recent study by *Monteiro et al.* [2011] has suggested that resource competition theory [*Tilman*, 1977] can help us begin to understand the regional distribution of diverse diazotroph communities and here we have expanded on that theme.

[56] We have examined the interplay between marine ecosystem structure, iron concentrations, and iron supply in the context of the Pacific ocean of a global three-dimensional ocean model with explicit representation of several types of nondiazotrophic and diazotrophic phytoplankton. We explore how the availability of iron critically regulates the ecosystem structure in the modeled low seasonality Pacific, and how the ecosystem itself controls iron concentrations.

[57] The model results, together with the framework of resource competition, suggest that diazotrophs only exist where nondiazotrophic phytoplankton are nitrogen limited *and* where the source of iron relative to the source of fixed nitrogen (excluding nitrogen fixed by diazotrophs) is greater than the ratio of cellular iron to nitrogen of nondiazotrophs. These are a more formal representation of the findings of *Monteiro et al.* [2011], are consistent with observations [*Moore et al.*, 2009; *Church et al.*, 2008; *Mills et al.*, 2004; *Berman-Frank et al.*, 2007], and provide a solid mechanistic interpretation of nutrient control on diazotrophy.

[58] Our results reinforce the tight connection between iron supply, diazotroph habitat and, in turn, iron concentrations in low seasonality regions of the Pacific. From a biogeochemical modeling perspective this tight link suggests that we can not simulate ecosystems correctly before we have an adequate representation of iron supply, but also we will not be able to capture observed iron concentrations without successfully parameterizing the ecosystem structure and physiology. Changes to modeled diazotroph physiological parameters, such as nutrient half saturation constants (see experiment K_{Fe}Diaz) or growth rates, will change the models concentration of iron and the regional distribution of diazotrophs.

[59] Our results also suggest a delineation of the low latitude Pacific into three distinct biogeographical provinces whose boundaries are regulated by the relative supply of iron and nitrogen. These provinces differ in regard to whether diazotrophs can exist or not, which phytoplankton type controls the iron concentration, and the biogeochemical response to changes in aeolian iron source. We suggest that separating the ocean into provinces in this manner provides a framework to delineate the regional varying controls on biogeochemistry and ecosystem structure. With an understanding of how provinces boundaries may change, we can potentially anticipate the biological and chemical shifts in past and future oceans.

[60] Though we have concentrated on the Pacific, these results apply also to other oceanic regions where nitrogen and iron are the key limiting regions. However in other regions of the ocean, especially those replete in iron, phosphorus takes on a more regulatory role [e.g., *Moore et al.*, 2009; *Mills et al.*, 2004]. This framework can also be extended to include phosphorus as a limiting nutrient, though it becomes significantly more complex. Here we have kept the framework as simple as possible as a first step in understanding the processes controlling the real ocean, and hence focused on the Pacific Ocean. This however does remain a modeling study that requires observational validation from, and could also potentially inform, future research cruises.

Appendix A: Additional Theoretical Consideration

[61] There is evidence that diazotrophs do not have to fix all the nitrogen they consume [see, e.g., *Holl and Montoya*, 2005]: We show here how this would affect the theoretical framework discussed in section 2. If we assumed that diazotrophs supplemented nitrogen fixation with nitrate uptake, and that diazotroph growth is still iron limited, equation (3) becomes:

$$\frac{dN}{dt} = -\mu_P \min\left(\frac{N}{N+\kappa_{NP}}, \frac{Fe}{Fe+\kappa_{FeP}}\right) P_P - \gamma\mu_D \frac{Fe}{Fe+\kappa_{FeD}} + m_D P_D + S_N$$

where γ is amount nitrate that diazotrophs consume ($\gamma = 0$ implies they fix all the nitrogen they require and $\gamma = 1$ implies they do not fix any nitrogen). The steady state nutrient concentration N^*, Fe^* are not altered, but the amount of nondiazotrophs in equations (7a) and (7b) (Table 1) becomes $P_P = \frac{S_N}{m_P} + (1-\gamma) m_D P_D$. This implies that the additional biomass fueled by presence of diazotrophs is limited to the amount of nitrogen they fix directly.

Appendix B: Ecosystem Model

[62] The ecosystem model equations are almost identical to those used and provided in detail by *Dutkiewicz et al.*

[2009]. Here we only present modifications relative to that paper. We present all parameter values used in these experiments in Tables 2 and 3, and refer the reader to *Dutkiewicz et al.* [2009] for fuller discussion of these.

[63] As it is computationally demanding to run ensembles of simulations for each sensitivity experiment (Table 4) with many tens of plankton as by *Dutkiewicz et al.* [2009] and *Monteiro et al.* [2011], we have reduced the model to using six phytoplankton functional types that are representative of the marine community found in those previous model studies.

[64] Phytoplankton growth is described by:

$$\mu_j = \mu_{\max_j} \gamma^T \gamma_j^I \gamma_j^N$$

where $\mu_{\max_j}$ is the maximum growth rate of phytoplankton j, and γ^T, γ_j^I, γ_j^N are the functions modulating growth due to temperature, light and nutrient availability respectively. γ_j^I and γ_j^N are as given by *Dutkiewicz et al.* [2009], but temperature modification is changed from that used by *Dutkiewicz et al.* [2009], and is based on the Arrenhius function [*Kooijman*, 2000]:

$$\gamma^T = \tau_1 \exp\left(A_E\left(\frac{1}{T+273.15} - \frac{1}{T_o}\right)\right)$$

where coefficients τ_1,A_E and T_o regulate the form of the temperature modification function. T is the local model ocean temperature. Here with only few phytoplankton types we do not specify specific ranges of temperatures as by *Dutkiewicz et al.* [2009]. The same temperature function (γ^T) is now also applied to the zooplankton maximum grazing rate and the organic matter remineralization rate.

[65] The iron model we use is based on that of *Parekh et al.* [2004, 2005] and *Dutkiewicz et al.* [2005]. We explicitly model the complexation of iron with an organic ligand, and assume that only free iron (Fe') can be scavenged, $c_{scav}Fe'$. As a modification relative to work by *Dutkiewicz et al.* [2009], we parameterize the scavenging as a function of the concentration of particulate organic carbon (POC) based on empirical data found for Thorium [*Honeyman et al.*, 1988] (a similar approach was used by *Parekh et al.* [2005]):

$$c_{scav} = c_o (POC)^{\phi}$$

where c_o determines maximum scavenging rate for iron, and ϕ empirically determined constant.

[66] An additional change in the iron cycle parameterization is a sedimentary source (F_{sed}) which is parameterized as a function of the sinking organic matter reaching the ocean bottom as suggested by the measurements of *Elrod et al.* [2004].

$$F_{sed} = R_{sed} \frac{\partial w_{POM} POP}{\partial z}$$

where R_{sed} is the ratio of sedimentary iron to sinking organic matter. This parameterization is applied in the grid cell just above the sea bottom everywhere.

[67] In previous simulations [e.g., *Dutkiewicz et al.*, 2009; *Monteiro et al.*, 2011] we used iron dust estimates from *Mahowald et al.* [2003] and assumed a constant solubility of iron dust. However field measurements suggest that iron has a large range of solubility which appears to vary regionally [e.g., *Chen and Siefert*, 2004; *Mahowald et al.*, 2009] perhaps dues to residence times and different chemical processes in the atmosphere [*Baker and Jickell*, 2006; *Luo et al.*, 2008]. Here we use the more recent modeled supply of bio-available aeolian iron dust of *Luo et al.* [2008] which include estimates of the soluble fraction of both natural and combustion sources. Together with the sedimentary sources also included in this version of the model, we have improved iron fields in the model relative to *Dutkiewicz et al.* [2009] and *Monteiro et al.* [2010, 2011], in particular, increased iron in the south subtropical gyre in the Pacific Ocean. As a consequence the current model has higher diazotroph concentrations in those regions which are closer to observations.

Appendix C: Additional Experiments

[68] We conducted several additional experiments that helped elucidate details of those discussed in the main text. Here we describe very briefly some of these simulations.

C1. Impact of Diazotrophy

[69] Diazotrophy is an important source of fixed nitrogen to the oceans. When we do not include diazotrophs in the model (Experiment NoDiaz), we find that there is a decrease in global primary production of about 8% relative to Control (Table 4). We note though that this represents an upper bound: Our model parameterizes that diazotrophs fix all the nitrogen they require, whereas if they were to only fix some nitrogen and consume nitrate for the rest, then the impact on the global primary production would be relatively lessened (see Appendix A).

[70] Biomass was lower in NoDiaz relative to Control in the regions where diazotrophs could exist, but also in nearby regions, suggesting that lateral supplies of newly fixed nitrogen were important. Iron concentrations in regions where diazotrophs survived in Control were significantly higher in NoDiaz, reinforcing the importance of the diazotrophs in controlling iron in these regions. We also conducted a simulation with no diazotroph and half the aeolian iron source (NoDiazLoIron). There was a 0.8% reduction in global primary production relative to NoDiaz, much smaller than the reduction seen between Control and LoIron (2.5%); the effect of reduced iron supply is much stronger in the presence of diazotrophs.

C2. Impact of Diversity in Diazotrophs

[71] *Monteiro et al.* [2010] included several diverse types of autotrophic diazotrophs which co-existed in some regions and out-competed each other in others. Here we include additional experiments where we include both unicellular diazotroph and *Trichodesmium*-analogs. The unicellular diazotrophs were conferred with lower nutrient requirements, $\kappa_{Fe_{unicellular}} < \kappa_{Fe_D}$ which leads to $Fe^*_{unicellular} < Fe^*_D$. Thus higher nitrogen fixation could be supported with the same iron supply and the regions where diazotrophy could be supported increased. In MultDiaz nitrogen fixation increased globally by 7% relative to the Control, and primary production increased globally by 1%. *Trichodesmium* and the unicellular diazotrophs contributed about equally to

the global total nitrogen fixation. In this experiment, the increased demand on phosphorus leads some small areas of the North Pacific to become phosphorus limited. Full understanding of the controls and response in these regions would require including a third nutrient in the theoretical framework, which is beyond the scope of this paper. However, in most regions similar patterns of nutrient and biomass changes are found relative to MultDiaz when we reduce the iron supply (MultDiazLoIron) to those seen in Figure 8.

C3. Iron Source Changes

[72] We also conducted additional experiments where we increased the aeolian dust source (by 4, DiazHiIron) and ran with the (lower) pre-industrial dust flux estimated by *Luo et al.* [2008] (DiazPreIron). Increasing the dust (DiazHiIron) led to substantial increase in nitrogen fixation (136TgN/y, a 58% increase relative to Control) and a 7% increase in primary production. In the high dust case, some regions of the Pacific became phosphorus limited. The difference between pre-industrial and modern dust fluxes leads to very similar results to those seen between LoIron and Control (Figure 8), and similar to those found by *Krishnamurthy et al.* [2009].

[73] **Acknowledgments.** The ocean circulation state estimates used in this study were provided by the ECCO Consortium (Estimating the Circulation and Climate of the Ocean) funded by the National Oceanographic Partnership Program (NOPP). We thank Patrick Heimbach in particular for his assistance. We are grateful to Natalie Mahowald for making the iron dust supply fields available. Comments from two anonymous reviewers helped improve this article. We are grateful for support from the Gordon and Betty Moore Foundation and NOAA.

References

Baker, A. R., and T. D. Jickells (2006), Mineral particle size as a control on aerosol iron solubility, *Geophys. Res. Lett.*, *33*, L17608, doi:10.1029/2006GL026557.

Behrenfeld, M. J., and P. G. Falkowski (1997), Photosynthetic rates derived from satellite-based chlorophyll concentration, *Limnol. Oceanogr.*, *42*, 1–20.

Berman-Frank, I., A. Quigg, Z. Finkel, A. J. Irwin, and L. Haramaty (2007), Nitrogen-fixing strategies and Fe requirements in cyanobacteria, *Limnol. Oceanogr.*, *52*, 2260–2269.

Bonnet, S., et al. (2008), Nutrient limitation of primary productivity in the Southeast Pacific (BIOSOPE cruise), *Biogeosciences*, *5*, 215–225

Boyd, P. W., et al. (2007), Mesoscale iron enrichment experiments 1993–2005: Synthesis and future directions, *Science*, *315*, 612–617, doi:10.1126/science.1131669.

Capone, D. G., J. P. Zehr, H. W. Paerl, B. Bergman, and E. J. Carpenter (1997), *Trichodesmium*, a globally significant marine cyanobacterium, *Science*, *276*, 1221–1229.

Chen, Y., and R. L. Siefert (2004), Seasonal and spatial distributions and dry deposition fluxes of atmospheric total and labile iron over the tropical and subtropical North Atlantic Ocean, *J. Geophys. Res.*, *109*, D09305, doi:10.1029/2003JD003958.

Church, M. J., K. M. Bjorkman, D. M. Karl, M. A. Saito, and J. P. Zehr (2008), Regional distributions of nitrogen-fixing bacteria in the Pacific Ocean, *Limnol. Oceanogr.*, *53*(1), 63–77.

de Baar, H. J. W., et al. (2005), Synthesis of iron fertilization experiments: From the Iron Age in the Age of Enlightenment. *J. Geophys. Res.*, *110*, C09S16, doi:10.1029/2004JC002601.

Deutsch, C., J. L. Sarmiento, D. M. Sigman, N. Gruber, and J. P. Dunne (2007), Spatial coupling of nitrogen inputs and losses in the ocean, *Nature*, *445*, 163–167.

Dutkiewicz, S., M. Follows, and P. Parekh (2005), Interactions of the iron and phosphorus cycles: A three-dimensional model study, *Global Biogeochem. Cycles*, *19*, GB1021, doi:10.1029/2004GB002342.

Dutkiewicz, S., M. Follows, and J. Bragg (2009), Modeling the coupling of ocean ecology and biogeochemistry, *Global Biogeochem. Cycles*, *23*, GB4017, doi:10.1029/2008GB003405.

Elrod, V. A., W. M. Berelson, K. H. Coale, and K. S. Johnson (2004), The flux of iron from continental shelf sediments: A missing source for global budgets, *Geophys. Res. Lett.*, *31*, L12307, doi:10.1029/2004GL020216.

Falkowski, P. G. (1997), Evolution of the nitrogen cycle and its influence on the biological sequestration of CO_2 in the ocean, *Nature*, *387*, 272–275.

Follows, M. J., S. Dutkiewicz, S. Grant, and S. W. Chisholm (2007), Emergent biogeography of microbial communities in a model ocean, *Science*, *315*, 1843–1846.

Garcia, H. E., R. A. Locarnini, T. P. Boyer, and J. I. Antonov (2006), *World Ocean Atlas 2005*, vol. 4, *Nutrients (Phosphate, Nitrate, Silicate), NOAA Atlas NESDIS*, vol. 64, edited by S. Levitus, 396 pp., NOAA, Silver Spring, Md.

Goebel, N., C. A. Edwards, B. J. Carter, K. M. Achilles, and J. P. Zehr (2008), Growth and carbon content of three different-sized diazotrophic cyanobacteria observed in the subtropical North Pacific, *J. Phycol.*, *44*, 1212–1220.

Gruber, N. (2004), The dynamics of the marine nitrogen cycle and its influence on atmospheric CO_2 variations, in *The Ocean Carbon Cycle and Climate*, *NATO Sci. Ser.*, vol. 40, edited by M. Follows and T. Oguz, pp. 97–148, Kluwer Acad., Dordrecht, Netherlands.

Holl, C. M., and J. P. Montoya (2005), Interactions between nitrate uptake and nitrogen fixation in continuous cultures of the marine diazotroph *Trichodesmium* (Cyanobacteria), *J. Phycol.*, *41*, 1178–1183.

Honeyman, B., L. Balistrieri, and J. Murray (1988), Oceanic trace metal scavenging and the importance of particle concentration, *Deep Sea Res., Part I*, *35*, 227–246.

Kooijman, S. A. L. M. (2000), *Dynamic Energy and Mass Budget in Biological Systems*, Cambridge Univ. Press, Cambridge, U. K.

Krishnamurthy, A., J. K. Moore, N. Mahowald, C. Luo, S. C. Doney, K. Lindsay, and C. S. Zender (2009), Impacts of increasing anthropogenic soluble iron and nitrogen deposition on ocean biogeochemistry, *Global Biogeochem. Cycles*, *23*, GB3016, doi:10.1029/2008GB003440.

Kustka, A., S. Sanudo-Wilhelmy, E. J. Carpenter, D. G. Capone, and J. A. Raven (2003), A revised estimate of the iron efficiency of nitrogen fixation with special reference to the marine cyanobacterium *Trichodesmium* spp. (cyanophyta), *J. Phycology*, *39*, 12–25.

LaRoche, J., and E. Breitbarth (2005), Importance of the diazotrophs as a source of new nitrogen in the ocean, *J. Sea Res.*, *53*, 67–91.

Luo, C., N. Mahowald, T. Bond, P. Y. Chuang, P. Artaxo, R. Siefert, Y. Chen, and J. Schauer (2008), Combustion iron distribution and deposition, *Global Biogeochem. Cycles*, *22*, GB1012, doi:10.1029/2007GB002964.

Mague, T. H., N. M. Weare, and O. Holm-Hansen (1974), Nitrogen fixation in the North Pacific Ocean, *Mar. Biol.*, *24*, 109–119.

Mahowald, N., and C. Luo (2003), A less dusty future?, *Geophys. Res. Lett.*, *30*(17), 1903, doi:10.1029/2003GL017880.

Mahowald, N., C. Lou, J. del Corral, and C. S. Zender (2003), Interannual variability in atmospheric mineral aerosols from a 22-year model simulation and observational data, *J. Geophys. Res.*, *108*(D12), 4352, doi:10.1029/2002JD002821.

Mahowald, N. M., D. R. Muhs, S. Levis, P. J. Rasch, M. Yoshioka, C. S. Zender, and C. Luo (2006), Change in atmospheric mineral aerosols in response to climate: Last glacial period, preindustrial, modern, and doubled carbon dioxide climates, *J. Geophys. Res.*, *111*, D10202, doi:10.1029/2005JD006653.

Mahowald, N., et al. (2009), Atmospheric iron deposition: Global distribution, variability and human perturbations, *Annu. Rev. Mar. Sci.*, *1*, 245–278, doi:10.1146/annurev/marine.010908.163727.

Margalef, R. (1968), *Perspectives in Ecological Theory*, 111 pp., Univ. of Chicago Press, Chicago, Ill.

Marshall, J. C., C. Hill, L. Perelman, and A. Adcroft (1997), Hydrostatic, quasi-hydrostatic and nonhydrostatic ocean modeling, *J. Geophys. Res.*, *102*(C3), 5,733–5,752.

Mills, M. M., C. Ridame, M. Davey, J. La Roche, and R. J. Geider (2004), Iron and phosphorus co-limit nitrogen fixation in the eastern tropical North Atlantic, *Nature*, *429*, 292–294.

Monteiro, F., M. J. Follows, and S. Dutkiewicz (2010), Distribution of diverse nitrogen fixers in the global ocean, *Global Biogeochem. Cycles*, *24*, GB3017, doi:10.1029/2009GB003731.

Monteiro, F. M., S. Dutkiewicz, and M. J. Follows (2011), Biogeographical controls on the marine nitrogen fixers, *Global Biogeochem. Cycles*, *25*, GB2003, doi:10.1029/2010GB003902.

Moore, C. M., et al. (2009), Large-scale distribution of Atlantic nitrogen fixation controlled by iron availability, *Nat. Geosci.*, *2*, 867–871, doi:10.1038/NGEO667.

Moore, J. K., and O. Braucher (2008), Sedimentary and mineral dust sources of dissolved iron to the world ocean, *Biogeosciences*, *5*, 631–656.

Moore, J. K., and S. C. Doney (2007), Iron availability limits the ocean nitrogen inventory stabilizing feedbacks between marine denitrification and nitrogen fixation, *Global Biogeochem. Cycles*, *21*, GB2001, doi:10.1029/2006GB002762.

Moore, J. K., S. C. Doney, and K. Lindsay (2004), Upper ocean ecosystem dynamics and iron cycling in a global three- dimensional model, *Global Biogeochem. Cycles*, *18*, GB4028, doi:10.1029/2004GB002220.

Moore, J. K., S. C. Doney, K. Lindsay, N. Mahowald, and A. F. Michaels (2006), Nitrogen fixation amplifies the ocean biogeochemical response to decadal timescale variations in mineral dust deposition, *Tellus*, *58B*, 560–572.

Parekh, P., M. J. Follows, and E. A. Boyle (2004), Modeling the global ocean iron cycle, *Global Biogeochem. Cycles*, *18*, GB1002, doi:10.1029/2003GB002061.

Parekh, P., M. J. Follows, and E. A. Boyle (2005), Decoupling of iron and phosphate in the global ocean, *Global Biogeochem. Cycles*, *19*, GB2020, doi:10.1029/2004GB002280.

Saba, V. S., et al. (2010), Challenges of modeling depth-integrated marine primary productivity over multiple decades: A case study at BATS and HOT, *Global Biogeochem. Cycles*, *24*, GB3020, doi:10.1029/2009GB003655.

Tagliabue, A., L. Bopp, O. Aumont, and K. R. Arrigo (2009), Influence of light and temperature on the marine iron cycle: From theoretical to global modeling, *Global Biogeochem. Cycles*, *23*, GB2017, doi:10.1029/2008GB003214.

Tegen, I., M. Werner, S. P. Harrison, and K. E. Kohfeld (2004), Relative importance of climate and land use in determining present and future global soil dust emission, *Geophys. Res. Lett.*, *31*, L05105, doi:10.1029/2003GL019216.

Tilman, D. (1977), Resource competition between planktonic algae: An experimental and theoretical approach, *Ecology*, *58*, 338–348.

Tilman, D. (1982), *Resource Competition and Community Structure*, *Monogr. Popul. Biol.*, vol. 17, 296 pp., Princeton Univ. Press, Princeton, N. J.

Uitz, J., H. Claustre, B. Gentili, and D. Stramski (2010), Phytoplankton class-specific primary production in the world's oceans: Seasonal and interannual variability from satellite observations, *Global Biogeochem. Cycles*, *24*, GB3016, doi:10.1029/2009GB003680.

Verdy, A., M. Follows, and G. Flierl (2009), Evolution of phytoplankton cell size in an allometric model, *Mar. Ecology Prog. Ser.*, *379*, 1–12.

Westberry, T., M. J. Behrenfeld, D. A. Siegel, and E. Boss (2008), Carbon-based primary productivity modeling with vertically resolved photoacclimation, *Global Biogeochem. Cycles*, *22*, GB2024, doi:10.1029/2007GB003078.

Wunsch, C., and P. Heimbach (2007), Practical global ocean state estimation, *Physica D*, *230*, 197–208.

S. Dutkiewicz, M. J. Follows, and B. A. Ward, Department of Earth, Atmospheric and Planetary Sciences, Massachusetts Institute of Technology, 77 Massachusetts Ave., Cambridge, MA 02139, USA. (stephd@ocean.mit.edu; mick@ocean.mit.edu; benw@mit.edu)

F. Monteiro, School of Geographical Sciences, University of Bristol, Bristol BS8 1SS, UK. (f.monteiro@bristol.ac.uk)